Journal of Physiology - Paris 104 (2010) 137–146

Contents lists available at ScienceDirect

Journal of Physiology - Paris

journal homepage: www.elsevier.com/locate/jphysparis

Recurrent spatiotemporal firing patterns in large spiking neural networks with ontogenetic and epigenetic processes

Javier Iglesias [a,b,c,*], Alessandro E.P. Villa [b,c]

[a] Departament de Física i Enginyeria Nuclear, Universitat Politècnica de Catalunya, Terrassa, Spain
[b] Grenoble Institut des Neurosciences (GIN), INSERM, UMR_S 836, NeuroHeuristic Research Group, Université Joseph Fourier, Grenoble, France
[c] Neuroheuristic Research Group, Information Systems Department ISI, University of Lausanne, Switzerland

ARTICLE INFO

Keywords:
Apoptosis
Spike timing dependent plasticity
Synaptic pruning
Preferred firing sequence

ABSTRACT

Neural development and differentiation are characterized by an overproduction of cells and a transient exuberant number of connections followed by cell death and selective synaptic pruning. We simulated large spiking neural networks (10,000 units at its maximum size) with and without an ontogenetic process corresponding to a brief initial phase of apoptosis driven by an excessive firing rate mimicking cell death due to glutamatergic neurotoxicity and glutamate-triggered apoptosis. This phase was followed by the onset of spike timing dependent synaptic plasticity (STDP), driven by spatiotemporal patterns of stimulation. Despite the reduction in cell counts the apoptosis tended to increase the excitatory/inhibitory ratio because the inhibitory cells were affected at first. Recurrent spatiotemporal firing patterns emerged in both developmental condition but they differed in dynamics. They were less numerous but repeated more often after apoptosis. The results suggest that initial cell death may be necessary for the emergence of stable cell assemblies, able to sustain and process temporal information, from the initially randomly connected networks.

1. Introduction

The pattern of neuronal connectivity in an adult brain is determined by the complex interplay of genetic expression, developmental maturation and by epigenetic processes associated to plasticity and learning. The overproduction of synaptic contacts during the early stages of neural development followed by massive synaptic pruning, persistence of high density of synapses until sexual maturation and decrease at the adult age appear to be a common pattern of Mammals (Huttenlocher, 1979; Oppenheim, 1981; Huttenlocher et al., 1982; Rakic et al., 1986; Rakic et al., 1994; Innocenti, 1995). In the cerebral cortex there are known regional differences in the timing of developmental brain plasticity that occurs earliest in the primary motor and sensory areas and latest in prefrontal cortex (Conel, 1939–1963; Huttenlocher and Dabholkar, 1997) thus suggesting a gradient-like organization during early corticogenesis (Elston, 2002; Fujita, 2002) that is likely to be related to cortical patterns of gene expressions (Yamamori and Rockland, 2006). The exuberant development of neural circuits involves the formation of long transient axonal projections, the overproduction of axonal branches and synapses and the overproduction of dendritic branches and/or spines. These features are strongly associated to the amount of living neurons because it is known that about less than half of the neurons survive during development till adulthood (Yuan et al., 2003; Innocenti and Price, 2005).

Apoptosis is the programmed cell death that has been observed ubiquitously in the nervous system which results in the massive loss of the cells and of all their appendices and synapses. It declines significantly during the postnatal period (Rice and Barone, 2000; Levitt, 2003). Developmental apoptosis is likely to be regulated by a combination of genetic, molecular (guidance and growth factors) and cellular mechanisms (Oppenheim, 1991; Luo and O'Leary, 2005; Low and Cheng, 2006). In particular, apoptosis has been associated with neurotoxicity mediated by excessive levels of glutamate (Kure et al., 1991; Bonfoco et al., 1995; Figiel and Kaczmarek, 1997). Glutamate is an amino acid that plays an essential role in neurotransmission in the CNS (Cotman and Monaghan, 1988). The activation of *N*-methyl-D-aspartate (NMDA) subclass of ionotropic glutamate receptor (NMDAR) is involved in synaptic plasticity (Roberts and Bell, 2002; Gerkin et al., 2007; Urakubo et al., 2008) as well as in neurotoxicity (Choi et al., 1988; Johnston et al., 2001). NMDA-mediated apoptosis is well recognized (Kure et al., 1991; Jiang et al., 2000; Zieminska et al., 2003). There

* Corresponding author. Address: Departament de Física i Enginyeria Nuclear, Universitat Politècnica de Catalunya, Terrassa, Spain.
E-mail addresses: javier.iglesias@upc.edu (J. Iglesias), alessandro.villa@neuroheuristic.org (A.E.P. Villa).

0928-4257/$ - see front matter © 2009 Elsevier Ltd. All rights reserved.
doi:10.1016/j.jphysparis.2009.11.016

is evidence that expression of apoptotic and antiapoptotic proteins (Schelman et al., 2004) and the effect of growth factors (Egawa-Tsuzuki et al., 2004) could be both regulated by glutamate but the exact mechanism underlying NMDA-mediated apoptosis is not yet fully understood.

The projections that are maintained after the initial massive cell death may proliferate and form transient collaterals that further extend in the target areas but that eventually tend be removed following a mechanism that is likely to be activity-dependent (Innocenti, 1995; Lopez-Bendito and Molnar, 2003). There are controversial results about the respective roles of pre- and post-synaptic activities in determining the establishment of connections rather than their selection but there is little doubt that selective patterns of activity, in addition to background activity, are necessary to achieve correctly this developmental phase (Shatz, 1990; Catalano and Shatz, 1998; Hanson and Landmesser, 2004; Mizuno et al., 2007).

Synaptic pruning – the elimination of synapses – is likely to deeply affect the information processing by differentiating the strength of the connections between neuronal populations. Spike timing dependent synaptic plasticity (STDP) is a change in the synaptic strength based on the ordering of pre- and post-synaptic spikes (Bell et al., 1997; Roberts and Bell, 2002; Karmarkar and Buonomano, 2002). It has been proposed as a mechanism to explain the strengthening of synapses repeatedly activated shortly before occurrences of spikes in the post-synaptic cells. STDP may also explain the weakening of synaptic strength whenever the pre-synaptic cell is repeatedly activated shortly after the occurrence of a post-synaptic spike. The study of the relation between synaptic efficacy and synaptic pruning suggests that the weak synapses may be modified and removed through competitive "learning" rules (Chechik et al., 1999). Then, such remodeling of neural wiring appears to be selective in the sense that converging synapses are competing for control of the timing of post-synaptic action potentials (Guyonneau et al., 2005).

The function achieved by the elimination of the exuberant synapses might relate to the emergence of selective properties of the surviving neural circuits (Chen et al., 2005; Iglesias et al., 2005). One such property could be the ability to preserve accurate temporal information distributed across a circuit of functionally interconnected neurons, referred to as "cell assembly". Cell assemblies interconnected in this way would be characterized by recurrent, above chance levels, ordered sequences of precise (in the order of few ms) interspike intervals referred to as spatiotemporal patterns of discharges or preferred firing sequences (Abeles, 1991). Such precise firing patterns have been associated with specific behavioral processes in rats (Villa et al., 1999) and primates (Shmiel et al., 2006).

We have extended our previous model (Iglesias and Villa, 2006; Iglesias and Villa, 2007) by the sequential implementation of several developmental processes that are directly inspired by the observation of neural development. In particular we introduced an "early developmental phase" characterized by cell death followed by the enabling of the synaptic modification rules applied to excitatory–excitatory (*exc, exc*) and excitatory–inhibitory (*exc, inh*) connections. We have also extended the characterization of the spatiotemporal firing patterns timing structure. Several aspects of our simulation framework refer to genetic aspects that are not analyzed here because they are parts of a long standing research project (Sanchez et al., 2007) compatible with hardware implementation (Eriksson et al., 2003). The precise aim of the current study is to investigate whether or not, and under which conditions, there is a dynamics of occurrence of spatiotemporal patterns of activity in such developing artificial neural networks.

2. Methods

2.1. Proliferation and differentiation

We assume that the ontogenesis of a pseudo-cortical area is determined along a sequence of discrete steps occurring during embryonic development. Time zero T_0 of the ontogenesis was characterized by the appearance of the first neural stem cell. All other neural stem cells originated from the first one by mitotic divisions. The proliferation process was ended by time T_p. In the current simulation we assume that the neural tissue is laid down on a 100×100 2D lattice. During the next ontogenetic phase the neural stem cells differentiated into several types of neurons.

In this study we set only two types of neurons: glutamatergic and GABAergic. We assume that no developmental "diseases" occurred during these phases such that out of a total amount of 10,000 neurons the two neuronal populations were divided in 8000 glutamatergic and 2000 GABAergic cells. The spatial distribution of these two populations followed a space-filling quasi-random Sobol distribution (Press et al., 1992). Two sets of 400 glutamatergic cells (i.e., 800 units overall), labeled sets *A* and *B*, were further differentiated. The units belonging to sets *A* and *B* correspond to the "sensory units" of the network – the input layer – meaning that in addition to sending and receiving connections from the other units of both types they received inputs from the ascending sensory pathway. Fig. 1 illustrates these early ontogenetic phases.

2.2. Synaptogenesis

For sake of simplicity the input layer of the network is represented on one side of the lattice in Fig. 2a but this figure panel is equivalent to Fig. 1d. At time T_{d2} the main differentiation phase ended and we assume that morphogenetic processes (e.g., based on diffusion of growth factors) were responsible to drive the establishment of connections – synaptogenesis – between the neurons

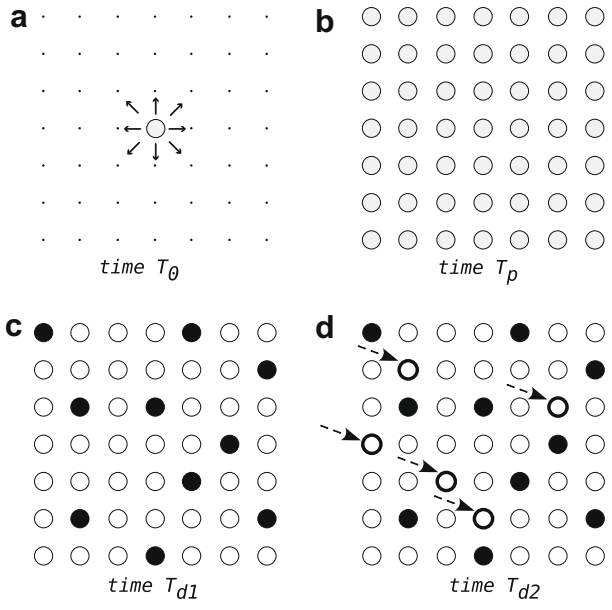

Fig. 1. Early embryonic phases of simulated ontogenesis of a pseudo-cortical area. (a) At time T_0 a neural stem cell begins to proliferate until. (b) Time T_p when a $N \times N$ lattice is filled. (c) By time T_{d1} the stem cells differentiated in two groups, glutamatergic (white circles) and GABAergic (black circles). (d) By time T_{d2} a certain number of glutamatergic cells (solid white circles) differentiated further to receive inputs from the ascending sensory pathway (dotted arrow).

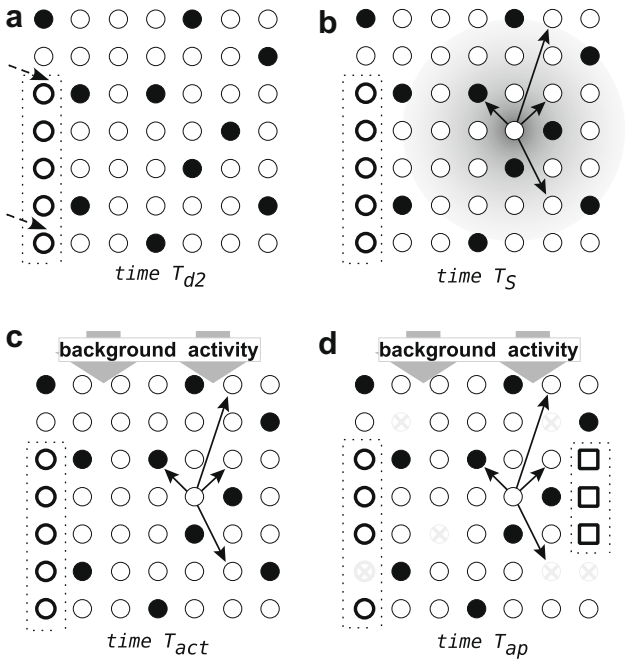

Fig. 2. Developmental phases of simulated ontogenesis of a pseudo-cortical area. (a) At time T_{d2} the glutamatergic cells (solid white circles) receiving projections from the ascending sensory pathway (dotted arrow) are represented on one side of the network but in reality they are scattered throughout the network. (b) Time T_S characteristic of the synaptogenesis. (c) The cellular development of the neurons is complete; the background activity provokes spiking activity in the network. (d) Time T_{ap} a massive cell death occurred and the dead cells (grey crossed circles) disappear; notice that some excitatory cells (solid squares) kept long range projections outside the local area.

of both populations. In the current study sparse connections between the populations of units were randomly generated according to a 2D Gaussian density function with dense projections in a local neighborhood described elsewhere (Iglesias et al., 2005). Long-range excitatory projections were allowed with a probability of 2%. Notice that edge effects induced by the borders were limited by folding the network as a torus. Time T_S indicates the end of the synaptogenesis (Fig. 2b). At this time the network is characterized by its maximum degree of connectivity due to the large extent of exuberant connections. Here we assume that no new synapses will be formed during the simulation.

2.3. Neuromimetic model

At time T_{act} the neuronal membrane is characterized by all ionic channels that allow the generation of the action potentials. We assume that at this stage the neurons began to receive unspecific inputs that affected the excitability of their membrane (Fig. 2c). The "spontaneous activity" that is generated within the network is parameterized by $B_i(t)$ that is the background activity arriving to the ith cell. In this study each neuron received an independent Poissonian distributed train of background pulses with an average frequency of 5 spikes/s. More details about the effect of background activity in a similar framework are found in (Iglesias et al., 2005).

The neurons are considered to behave like leaky integrate-and-fire units whose neuromimetic model is briefly described as follows. At each time step, the value of the membrane potential of the ith unit, $V_i(t)$, is calculated such that

$$V_i(t+1) = V_{\text{rest}[q]} + B_i(t) + (1 - S_i(t))((V_i(t) - V_{\text{rest}[q]})k_{\text{mem}[q]}) + \sum_j w_{ji}(t)$$

where $V_{\text{rest}[q]}$ corresponds to the value of the resting potential for the units of type $[q]$, $B_i(t)$ the background activity arriving to the ith unit, $S_i(t)$ the state of the unit, $k_{\text{mem}[q]} = \exp(-1/\tau_{\text{mem}[q]})$ the constant associated to the current of leakage for the units of type $[q]$, and $w_{ji}(t)$ are the post-synaptic potentials of the jth units projecting to the ith unit.

The state of a unit $S_i(t)$ is a function of the membrane potential $V_i(t)$ and of a threshold $\theta_{[q]_i}$, such that $S_i(t) = \mathscr{H}(V_i(t) - \theta_{[q]_i})$, where $\mathscr{H}$ is the Heaviside function, $\mathscr{H}(x) = 0 : x < 0, \mathscr{H}(x) = 1 : x \geqslant 0$. It is assumed that a unit can generate a spike only for $S_i(t) = 1$. In addition, the state of the unit depends on the refractory period $t_{\text{refract}[q]}$: after spiking, the membrane potential was reset to its resting potential, and the unit entered an absolute refractory period lasting three and two time steps for glutamatergic and GABAergic units, respectively.

The type of the synapse is a parameter that depends on the neurotransmitter released by the pre-synaptic cell and by the receptor of the post-synaptic neuron. In the current study we assume that the activation of all glutamatergic receptors depolarized the membrane (i.e., they are excitatory). We assume also that all GABAergic receptors were associated to hyperpolarizing currents (i.e., they are inhibitory). Then, the glutamatergic cells are referred to as *excitatory cells* and the GABAergic cells as *inhibitory cells*. Furthermore, we assume that the excitatory post-synaptic potential of glutamatergic synapses on glutamatergic cells $P_{[glu.glu]}$ (*exc, exc*) and on GABAergic cells $P_{[glu.GABA]}$ (*exc, inh*) were similar. The same assumption is made for inhibitory post-synaptic potentials $P_{[GABA.glu]}$ (*inh, exc*) and $P_{[GABA.GABA]}$ (*inh, inh*). The synaptic weight w_{ji} is expressed by $w_{ji}(t+1) = S_j(t) \cdot A_{ji}(t) \cdot P_{[q_j.q_i]}$, where S_j is the state of the pre-synaptic unit, $P_{[q_j.q_i]}$ is the synaptic type, and A_{ji} is the activation level of the synapse discussed below in Section 2.5. In the current study a fixed activation level $A_{ji}(t) = 1$ was set for (*inh, exc*) and (*inh, inh*) synapses, with $P_{[GABA.x]} = -0.8$ mV. For all excitatory synapses the parameters were $A_{ji}(t) = 2$ and $P_{[glu.x]} = 0.84$ mV.

2.4. Massive cell death

The "death" of units is introduced in the current model and represents a major difference with our previous studies (Iglesias et al., 2005; Iglesias and Villa, 2007). Cell death may be directly provoked by a mechanism associated with glutamatergic neurotoxicity which, in our case, corresponds to the possibility to enter an apoptotic faith after an excessive firing rate. The second cause of cell death is indirect and it happened when a cell lost all its excitatory inputs. In all cases a dead unit was characterized by the absence of any spiking activity and its removal from the neuronal network computation.

The apoptotic phase started at T_{act}, when the units began to be depolarized by the background activity. The spiking activity of the excitatory neurons builded-up very fast due to the presence of the large amount of recurrent exuberant connections within the network. This excitatory activity provoked a rapid increase in the activity of the majority of the cells of the network. We assume that an extremely high level of activity is associated with high levels of glutamate. During this phase, at each time step and for each unit i, an average firing rate $FR_{50}(i)$ was computed over a running window corresponding to 50 ms. For both excitatory and inhibitory neurons a maximum firing rate *FRM* was arbitrarily determined following a parameter search procedure. In this study we used $FRM_{exc} = 245$ spikes/s and $FRM_{inh} = 250$ spikes/s, respectively. This maximum firing rate *FRM* is assumed to trigger the genetic expression leading to apoptosis. If $FR_{50} > FRM$ for the corresponding unit type the cell had a probability to enter apoptosis according to the function

$$P_{death}(t) = \frac{0.5 \cdot t^2 - 4.5 \cdot 10^{-6} \cdot t^3}{44 \cdot (2.5 \times 10^6 + 6 \times 10^{-3} \cdot t^2)}. \quad (1)$$

The parameters of this function are far from representing any known cellular behavior. The function of Eq. (1) was selected following a parameter search procedure aimed to maintain a balanced excitatory/inhibitory ratio despite the cell death affecting all populations of cells. The probability to enter apoptosis increased with time such that $P_{death}(t = 100\,\text{ms}) = 4.5 \times 10^{-5}$, $P_{death}(t = 700\,\text{ms}) = 2.2 \times 10^{-3}$ and $P_{death}(t = 800\,\text{ms}) = 2.9 \times 10^{-3}$. Notice that at the end of this phase a subpopulation of the excitatory cells is characterized by their projections outside the network area (Fig. 2). These long-term projecting cells are assumed to correspond to the "output layer" of the network, but they will not be discussed further in this paper.

2.5. Synaptic plasticity

The synaptic spike timing dependent plasticity (STDP) was enabled at the end of the apoptotic phase (Fig. 3b). It is assumed *a priori* that modifiable synapses are characterized by discrete activation levels (Montgomery and Madison, 2004; Genoux and Montgomery, 2007) that could be interpreted as a combination of two factors: the number of synaptic *boutons* between the pre- and post-synaptic units and the changes in synaptic conductance. A *real-valued variable* $L_{ji}(t)$ is used to implement the spike timing dependent plasticity rule for $A_{ji}(t)$, with integration of the timing of the pre- and post-synaptic activities. The variables $L_{ji}(t)$ are user-defined boundaries of attraction $L_0 < L_1 < L_2 < \cdots < L_{N-1} < L_N$ satisfying $L_{k-1} < [A_k] < L_k$ for $k = 1, \cdots, N$. This means that whenever $L_{ji} > L_k$ the activation variable A_{ji} jumps from state $[A_k]$ to $[A_{k+1}]$. Similarly, if $L_{ji} < L_k$ the activation variable A_{ji} jumps from state $[A_{k+1}]$ to $[A_k]$. Moreover, after a jump of activation level $[A]$ occurred at time t the real-valued variable L_{ij} is reset to $L_{ij}(t+1) = \frac{L_k + L_{k+1}}{2}$.

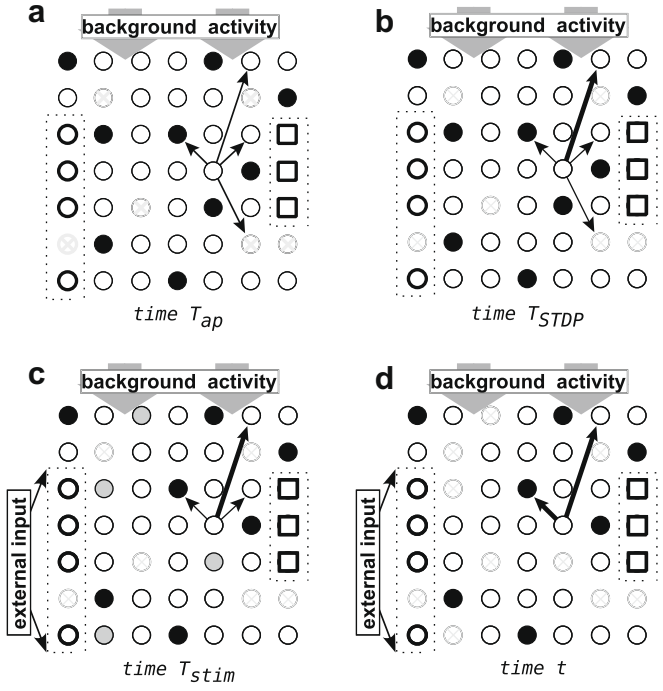

Fig. 3. Maturation phases of simulated ontogenesis of a pseudo-cortical area. (a) At time T_{ap} the massive cell death occurred and the dead cells (grey crossed circles) disappear. (b) At time T_{STDP} the processes characteristic of spike timing dependent plasticity began to modify the synaptic weights (different arrow thicknesses). (c) The external input reaches the input layer of the network at time T_{stim}; the synaptic pruning is affecting cells (grey circles) that remain without excitatory inputs. (d) At any time now synaptic and cell pruning are driven by STDP.

Spike timing dependent plasticity (STDP) defines how the value of L_{ji} at time t is changed by the arrival of pre-synaptic spikes, by the generation of post-synaptic spikes and by the correlation existing between these events. On the generation of a post-synaptic spike (i.e., when $S_i = 1$), the value L_{ji} receives an *increment* which is a decreasing function of the elapsed time from the previous pre-synaptic spike at that synapse. Similarly, when a spike arrives at the synapse, the variable L_{ji} receives a *decrement* which is likewise a decreasing function of the elapsed time from the previous post-synaptic spike (i.e., when $S_j = 1$). More details on the STDP rule can be found elsewhere (Iglesias et al., 2005).

The activation levels of *(exc, exc)* and *(exc, inh)* synapses were allowed to take one of the values $A_{ji}(t) = \{0, 1, 2, 4\}$. If $A_{ji}(t) = 0$ a projection was permanently pruned out. The projections from and to the units that died during the apoptotic phase underwent a decay of their synaptic weight without any chance of recovery, thus eventually leading to the cell pruning when the activation level of all their synapses reached $A_{ji}(t) = 0$. The loss of all excitatory inputs provoked the cell death and these units stopped firing (even in presence of background activity) immediately after the pruning of the last excitatory afference from within the network. It is important to notice that some units that survived the apoptotic phase could die at later time because they remain without viable excitatory inputs due to synaptic depression. Other projections could be pruned if synaptic depression driven by STDP occurred leading to $A_{ji}(t) = 0$ without necessarily leading to cell death. This is the phase when competition between the inputs occur and most of the exuberant connections disappear.

2.6. Content-related Stimuli

The first sensory inputs were fed into the network approximately at the same time (Fig. 3c) when spike timing dependent plasticity was enabled. Patterned activity organized both in time and space getting into the "input layer" of the network is assumed to correspond to content-related activity conveyed by the ascending sensory pathway and by activity generated elsewhere in the brain. Each stimulus lasted 100 ms and was followed by a period without stimulation that lasted 1900 ms (rate of stimulation was 0.5 stim/s).

The spatial organization of the stimulus was described elsewhere (Iglesias and Villa, 2007) and briefly summarized as follows. The sets A and B of units of the input layer were divided into 10 groups of 40 units each, $A = \{A_1, A_2, \ldots, A_{10}\}$ and $B = \{B_1, B_2, \ldots, B_{10}\}$. During the first millisecond of the AB stimulation all 40 units belonging to the set A_1 received a large depolarization that induced a spike if the unit was not in a refractory period. At the next millisecond each unit belonging to the set A_2 was strongly activated and so forth until the units of set A_{10} were activated. The entire sequence of activation A_1A_{10} lasted 10 ms and was repeated five times, followed by five times the entire sequence B_1B_{10}. A stimulus labeled BA was generated in a similar manner with five times the sequence B followed by five times the sequence A.

2.7. Spike train analysis

A spike train is composed by the time series of spike occurrences and is considered as a point process. Spike trains from all active cells were recorded for off-line analysis. The Poisson background noise alone could provoke a unit to fire whenever the excitability was close to the threshold. The other spikes were generated by the convergence of synchronous activity (i.e., temporal summation of excitatory post-synaptic potentials) generated within the network. In order to study the activity that is produced within

the simulated network those spikes associated to the background process were recorded separately and discarded from the raw spike trains such to extract the so-called "effective spike trains" (Hill and Villa, 1997).

The effective spike trains were searched for the occurrence of spatiotemporal firing patterns following the "pattern grouping algorithm" PGA (Tetko and Villa, 2001). For the present study, the pattern grouping algorithm was used to find patterns of at least 3 spikes (triplets), with a minimal significance level of 10%, repeating at least seven times in the interval [1–100] s, provided the entire pattern lasted not more than 800 ms and was repeated with an accuracy of ±5 ms.

3. Results

Each simulation run lasted 100,000 discrete time steps (T_{end}), with one time step corresponding to 1 ms in the model. The states (spiking/not spiking) of all units were updated synchronously. Starting at time zero and throughout all the simulation run each unit received a background activity following an independent Poisson process of 5 sp/s on average.

The early developmental phase, characterized by apoptosis began at time $t = 0$ and lasted until $t = T_{edp}$. Notice that the excitatory/inhibitory ratio was equal to 4/1 at $t = 0$. Two different durations of the early developmental phase were investigated here: $T_{edp} = 700$ and 800 time steps. The spike timing dependent plasticity was enabled at $t = T_{edp} + 1$. At time $t = 1001$ ms the first stimulation, lasting 100 ms, was applied, then until $t = 1100$ ms. Between $t = 1101$ ms and $t = 3000$ ms only the background activity was getting into the network. At time $t = 3001$ ms another stimulation was applied and so forth until the end of the simulation run. Overall this corresponded to 50 presentations of the stimulus along one simulation run. The stimuli *AB* and *BA* appeared in random order as described elsewhere (Iglesias and Villa, 2007). The simulated activity of one same network (i.e., generated by the same "genetic rules") was repeated five times using five different random generator seeds. Indeed, each seed produced different background activity that affected the early faith of cells and synaptic pruning. Each simulation run was performed with and without apoptosis and the corresponding effective spike trains were recorded and analyzed.

3.1. Activity-related cell death

Fig. 4 shows the evolution of the number of excitatory and inhibitory units during the initial 1000 time steps that followed the maximum development of the exuberant connectivity. During the first 800 time steps, all units with mean firing rates exceeding *FRM* could die by apoptosis with the probability expressed by $P_{\text{death}}(t)$ (Eq. (1)). The survival dynamics was linearly fit with the probability function and showed that the inhibitory units expressed the apoptotic behavior about 70 time steps earlier than the excitatory units. At time $t = 1000$ ms STDP-driven synaptic pruning was enabled. With STDP the synaptic weights could become so weak to provoke synaptic pruning and, in some cases, the loss of all excitatory inputs to a unit and its subsequent death at a longer time-scale.

The effect of a shorter period of apoptosis was studied only with $T_{edp} = 700$ time steps. Such shorter apoptotic phase provoked the death of 956 excitatory and 302 inhibitory units. With $T_{edp} = 800$ ms apoptosis affected 1355 excitatory and 416 inhibitory units. By the end of the apoptotic phase the ratio of excitatory/inhibitory units increased to 4.15/1 and 4.19/1 with T_{edp} equal to 700 and 800 time steps, respectively. The firing rate of all surviving excitatory units not belonging to the input layer was computed towards the end of each simulation run in the 1000 time steps interval immediately preceding the last stimulus presentation (i.e., between $T_{end} - 2000 < t < T_{end} - 1000$ ms).

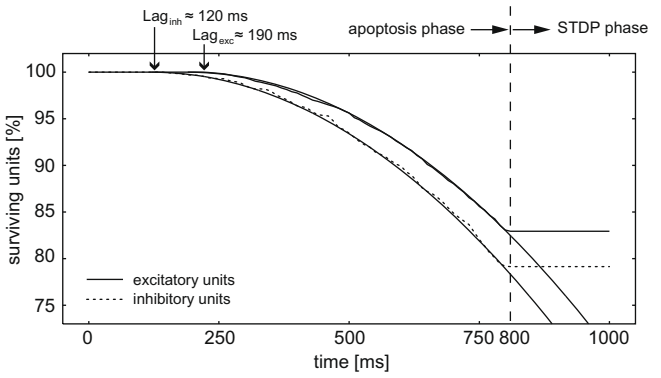

Fig. 4. Ratio of surviving units as a function of time with respect to initial conditions: 8000 excitatory units (plain line) and 2000 inhibitory units (dotted line). In this simulation, the apoptosis was stopped after 800 time steps ($T_{edp} = 800$). Thin lines correspond to the fitting against the probability function $P_{\text{death}}(t)$ with lags: 120 ms ($R^2 = 0.9797$) and 190 ms ($R^2 = 0.9902$) for the excitatory and inhibitory units, respectively.

The average activity (mean ± SEM) of the excitatory units was 4.6 ± 1.9 spikes/s with $T_{edp} = 700$ ms, and 5.0 ± 2.0 spikes/s with $T_{edp} = 800$ ms. In absence of any apoptosis the average activity was 4.3 ± 1.7 spikes/s. Fig. 5 shows the differential histogram (bin-to-bin difference) between the distributions of the firing rate in presence and in absence of apoptosis with $T_{edp} = 800$ ms. This histogram emphasizes the fact that almost 10% of the overall excitatory units shifted their firing rate from frequencies below 4 spikes/s to higher rates, thus accounting for the global increase of average activity mentioned above.

3.2. Spatiotemporal firing patterns

At time $t = T_{end}$ for each simulation run obtained with a different random generator seed we selected the units characterized by at least five active excitatory afferences from within the network but the input layer. These units were called *interconnected units*. The effect of introducing the apoptosis in the simulated neural development is summarized in Table 1. This table shows that the number of interconnected units decreased by almost half with apoptosis ($n = 578$ vs. 1180) despite the overall number of excitatory units decreased by 12%.

The effective spike trains of the interconnected units were searched for spatiotemporal firing patterns that repeated more

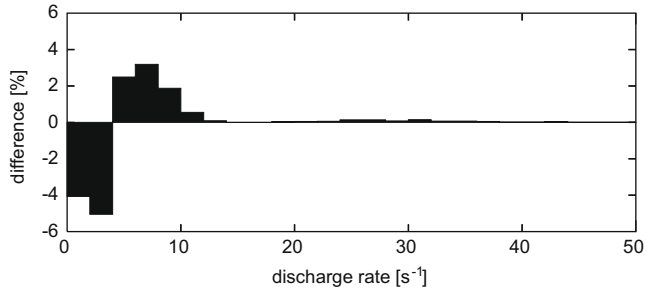

Fig. 5. Bin-to-bin difference of the distribution (relative frequency) of the neuronal firing rates recorded in the network that experienced apoptosis minus the distribution of firing rates of the very same network when apoptosis was not enabled. Bin size: 2 spikes/s. Notice that the apoptotic experience provoked a decrease in the number of neurons that fired less than 4 spikes/s and an increase in the number of those that fired between 6–12 and near 30 spikes/s.

Table 1
Cumulated data over five simulation runs obtained with different random generator seeds. The average data about recurrency, pattern duration and interspike intervals report mean ± SEM values per pattern.

Apoptosis	Enabled	Disabled
Total number of *exc* units	31710	36110
Interconnected units	578	1180
Total number of patterns	9	30
Triplets (*N*)	7	13
Pattern recurrency	56.6 ± 7.0	18.9 ± 5.5
Pattern duration (ms)	587.3 ± 58.5	583.8 ± 46.3
Interspike interval (ms)	293.6 ± 57.1	291.9 ± 34.2
Quadruplets (*N*)	2	17
Pattern recurrency	18.5	40.8±5.9
Pattern duration (*ms*)	766.5	591.5±33.8
Interspike interval (*ms*)	255.5	197.2±22.9

than seven times. All patterns except one were formed by occurrences of the same unit, referred to as single-unit patterns. In presence of apoptosis only nine patterns were found, seven corresponding to triplets and two to quadruplets (Table 1). The overall pattern duration was on average close to 580–590 ms in all experimental conditions. The variabilities of the pattern temporal structure (duration and interspike intervals) in presence of apoptosis were larger but not significantly different, maybe due to the small samples size. A relevant difference in spatiotemporal firing patterns dynamics with or without apoptosis lies in the average recurrency per pattern. Table 1 shows that in case apoptosis was present in the neural development a triplet repeated more than 50 times during one simulation run, while it repeated less than 20 times without apoptosis. This difference, although impressive, is yet not significant (χ^2-test) due to the small samples size.

Appearance and disappearance of patterns was due to developmental changes shaped by STDP in the network connectivity underlying the process of temporal information. Fig. 6 shows extreme cases of onset dynamics of single-unit patterns observed in the absence of apoptosis. In one case a triplet appeared early in the network maturation and disappeared after $t \approx 35,000$ ms (Fig. 6a and b). The single-unit pattern $\langle 148C, 148C, 148C;\ 191 \pm 0.9, 698 \pm 1.0\rangle$ was composed by spikes produced by unit #148C. This notation means that a precise firing sequence started with a spike of unit #148C, followed 191 ± 0.9 ms later by a second spike of the same unit, and followed by a third spike 698 ± 1.0 ms after the first. In the opposite case another pattern (a quadruplet in this example) appeared only at a later stage of maturation after $t \approx 65,000$ ms (Fig. 6c and d).

The simulation conditions with apoptosis during the early phase of the development did not produce such extreme appearance and disappearance lags. We selected one quadruplet and two triplets among the nine detected precise firing sequences to show representative features of patterned activity. The dynamics of the onset times of each pattern was studied at three developmental periods that we have arbitrarily subdivided as *early* ($1 \leqslant t < 50$ s), *mature* ($50 \leqslant t < 75$ s) and *late* ($75 \leqslant t < 100$ s).

The precise firing sequence $\langle 214F, 214F, 214F, 214F;\ 74 \pm 4.5, 682 \pm 2.5, 798 \pm 3.0\rangle$ was a single-unit pattern formed by spikes of unit #214F (Fig. 7a). Between $t = 1000$ ms and $t = T_{end}$, 17 repetitions of this pattern were observed. The statistical significance of the excess of pattern occurrence computed by the pattern grouping algorithm (Tetko and Villa, 2001) was $P = 3.9 \times 10^{-2}$. The autocorrelogram was always computed to determine if some strange internal dynamics could be at the origin of patterned activity. In general the autocorrelogram was characterized by a flat curve with an initial trough. The trough indicates a refractory period and the flatness of the curve indicates the tendency to fire following a Poissonian distribution and not in bursts. We looked for a potential correlation between the stimulus onset time and the onset times of the pattern occurrences. This pattern tended to appear in the 500 ms that immediately followed the stimulation onset (Fig. 7d) despite the fact that no sharp response was observed in the peristimulus time histogram (Fig. 7c).

Another interesting feature to observe in the quadruplet $\langle 214F, 214F, 214F, 214F;\ 74 \pm 4.5, 682 \pm 2.5, 798 \pm 3.0\rangle$ is the distribution of pattern onset times along the simulation run (Fig. 7e). We

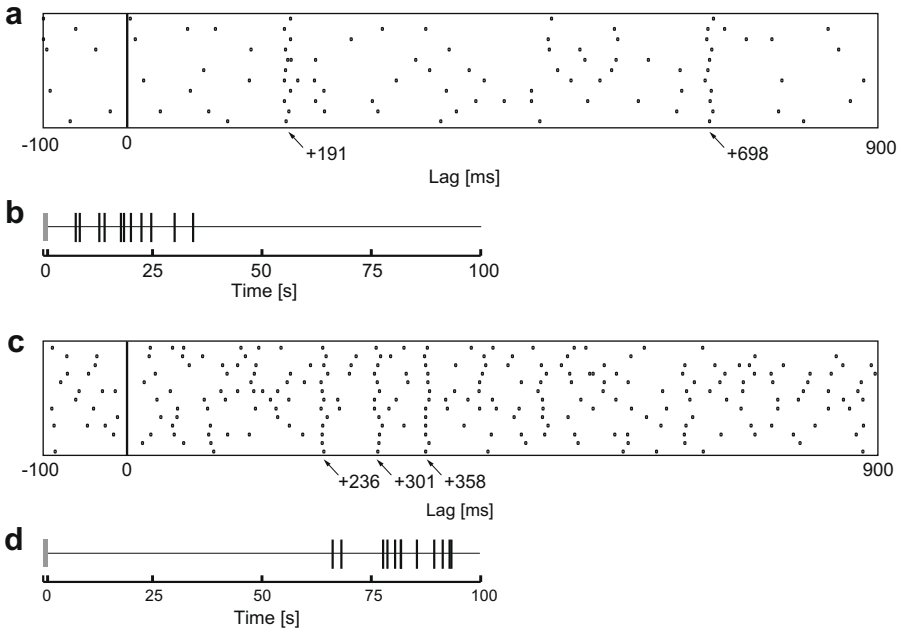

Fig. 6. Spatiotemporal firing pattern $\langle 148C, 148C, 148C;\ 191 \pm 0.9, 698 \pm 1.0\rangle$ that repeated 11 times in the absence of apoptosis. Unit #148C spontaneous mean firing rate: 4.0 spikes/s. Raster plot (a) of the patterns aligned on the pattern start and raster plot of patterns onset, (b) each vertical tick corresponds to the onset time of each pattern occurrence; Spatiotemporal firing pattern $\langle 554, 554, 554, 554;\ 236 \pm 0.7, 301 \pm 0.8, 358 \pm 0.6\rangle$ in the absence of apoptosis. Unit #554 spontaneous mean firing rate: 13.1 spikes/s. Raster plot (c) showing 13 repetitions and raster plot of pattern onset (d).

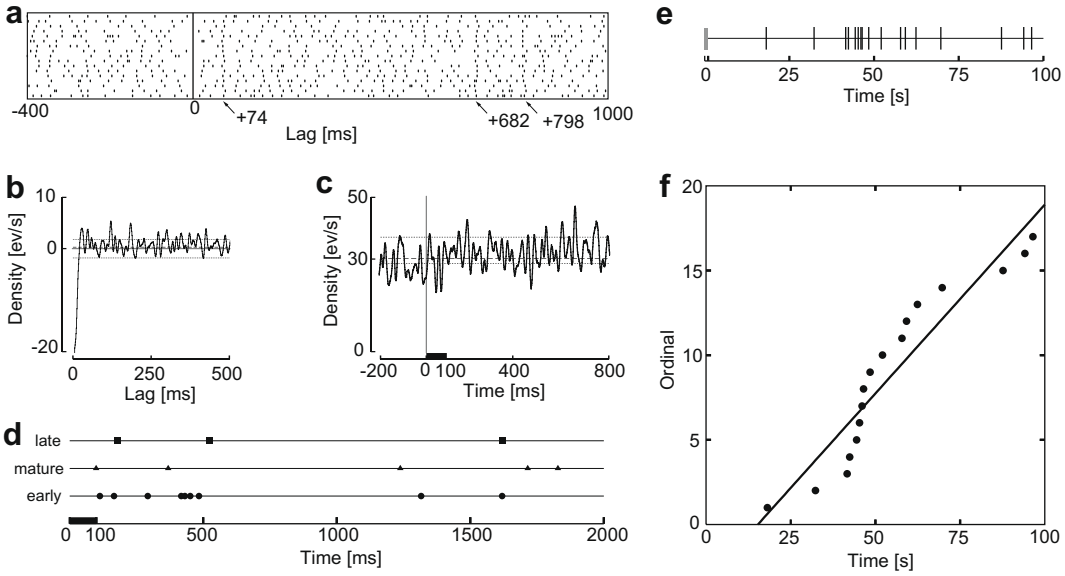

Fig. 7. Spatiotemporal firing pattern ⟨214F,214F,214F,214F; 74 ± 4.5,682 ± 2.5,798 ± 3.0⟩ that repeated 17 times in presence of apoptosis. Unit #214F spontaneous mean firing rate: 28.4 spikes/s. (a) Raster plot aligned on the pattern start. (b) Autocorrelogram recorded during 1000 ms preceding each stimuli onset, scaled in rate (events/s) vs. lag (ms). (c) Peri-event time histogram scaled in rate (events/s) vs. time (ms). The stimulus presentation (thick black line on the abscissa) started at time 0 and lasted 100 ms. (d) Peri-stimulus pattern plot shows the occurrences of pattern events (small vertical ticks) as a function of stimulus onset and of network developmental stage. Stimulus duration represented by the black line at the interval [0–100] ms. (e) Raster plot of pattern onset: each vertical tick represents the onset time of each pattern occurrence. (f) Pattern occurrence regression plot: each black dot represents the onset time of each pattern against its ordinal. The line represents the linear regression. The residuals of the regression are serially correlated and not randomly distributed around the regression line.

found that 9/17 occurrences occurred during the *early* ($t < 50$ s), five during the *mature* and three during the *late* period. One time in the interval [1–25] s, eight times in [25–50] s, and eight times in [50–100] s. This might suggest that the network dynamics giving rise to the pattern appeared early and was slowly disrupted by the continuous STDP-driven pruning. The distribution of pattern occurrences was tested against a linear regression with serial correlation between the residuals by the Durbin–Watson (DW) test (Durbin and Watson, 1971; Draper and Smith, 1998) characterized by a statistic value d and the sample size n. The smaller the value of d the stronger the serial correlation. Fig. 7f shows that the distribution of pattern occurrences is not regularly distributed along the regression line. Indeed DW-test ($d = 0.4864, n = 17$) indicates successive error terms are, on average, positively correlated with significance $P \ll 1\%$.

The pattern ⟨16A3,16A3,16A3; 274±4.5,708±1.5⟩ was observed 41 times (Fig. 8a) between $t = 1000$ ms and $t = T_{end} (P = 4.2 \times 10^{-2})$. This unit was clearly responsive to the stimulus as indicated by its peri-stimulus time histogram (Fig. 8c) but the pattern onset was not triggered by the stimulus (Fig. 8d). The pattern occurred more frequently towards the end of the simulation run, during the *mature* and *late* periods. This might suggest that the changes in the network dynamics, induced by the continuous STDP-driven pruning, lead to a transient state between 50 and 75 s when the appearance of this pattern was particularly favored. The linear regression on the pattern occurrence (Fig. 8f) was significant ($P \ll 1\%$) and the Durbin–Watson test on the residuals ($d = 0.3884, n = 41$) indicated that successive error terms were positively correlated ($P \ll 1\%$), too. Furthermore, notice that the patterns tended to occur in bursts.

The triplet ⟨BDC,BDC,BDC; 82 ± 3.5,687 ± 5.5⟩ recurred 56 times before T_{end} (Fig. 9a). with a high level of significancy ($P = 4.5 \times 10^{-5}$). The autocorrelogram (Fig. 9b) shows a broad hump after the initial trough due to the refractory period. This hump indicates a moderate tendency to fire in bursts. No correlation could be found between the timing of the spatiotemporal pattern and the stimulation onset (Fig. 9d). Conversely, the pattern occurred preferentially late in the simulation run (i.e., 12 times in the interval [1–50] s, 22 times in [50–75]s, and 22 times in [75–100]s, Fig. 9e). Serial correlation of the pattern occurrences was also revealed by the Durbin–Watson test on the residuals ($d = 0.1376, n = 56, P \ll 1\%$). This triplet is interesting not only for its high number of repetitions, but also for the fact that the network dynamics giving rise to its emergence was maintained for the last 50 s of simulation despite the continuous STDP-driven pruning. The raster plot (Fig. 9a) suggests even the "build-up" of a more complex pattern, starting at $t \approx 60000$ ms (horizontal arrow), that consisted in a superpattern with an additional event of unit #BDC that occurred approximately 300 ms (vertical arrow) before the triplet onset.

4. Discussion

We simulated a large scale spiking neural network characterized by a brief initial phase of apoptosis that extended our previous model (Iglesias and Villa, 2007). During this phase the units that exceeded a certain threshold of firing had an increasing probability to die with the passing of time until T_{edp} equal to 700 or 800 time units (depending on the simulation runs). The rationale of this rule is that a very high activity of the excitatory cells is assumed to release excessive levels of glutamate, which is the excitatory neurotransmitter considered in our simulations. Glutamate is not only known to provoke neurotoxicity (Choi et al., 1988) but is likely to be involved in triggering apoptosis (Jiang et al., 2000; Zieminska et al., 2003; Schelman et al., 2004). At the end of this apoptotic phase spike timing dependent plasticity (STDP) and synaptic pruning were enabled. Then, cell death could occur only if a unit became deafferented of its excitatory inputs after synaptic weights were depressed to zero following STDP. The comparisons of network activity were performed in presence of regular repetitions of a spatially and temporally organized external input (Iglesias and Villa, 2007).

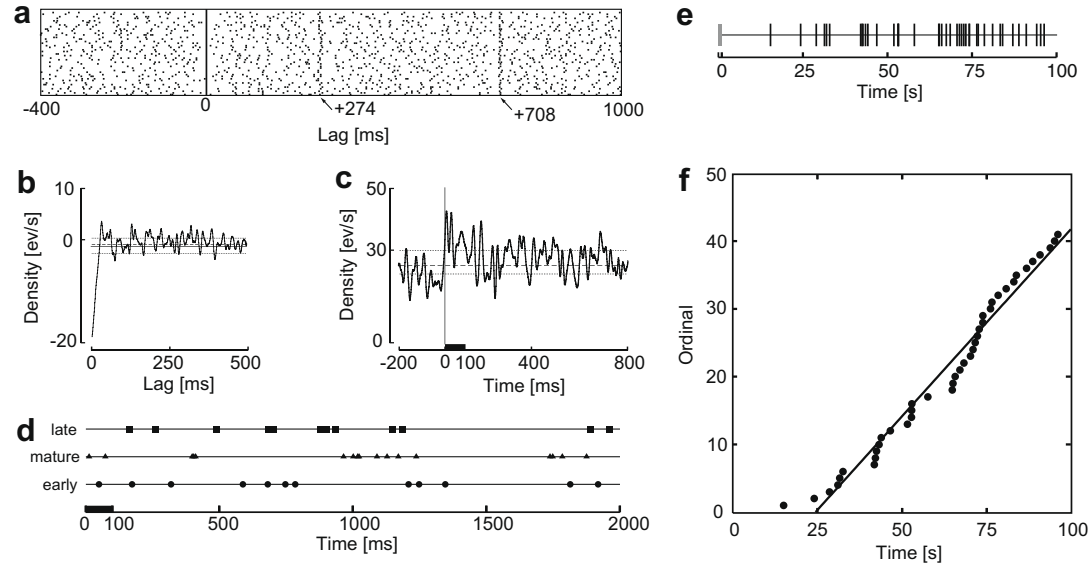

Fig. 8. Spatiotemporal firing pattern ⟨16A3, 16A3, 16A3; 274 ± 4.5, 708 ± 1.5⟩ that repeated 41 times in presence of apoptosis. Unit #16A3 spontaneous mean firing rate: 22.7 spikes/s. Raster plot aligned on the pattern start (a), autocorrelogram (b), peri-event time histogram (c), peri-stimulus pattern plot (d), raster plot of pattern onset (e), and pattern occurrence regression plot (f). See figure for more details of panels layout.

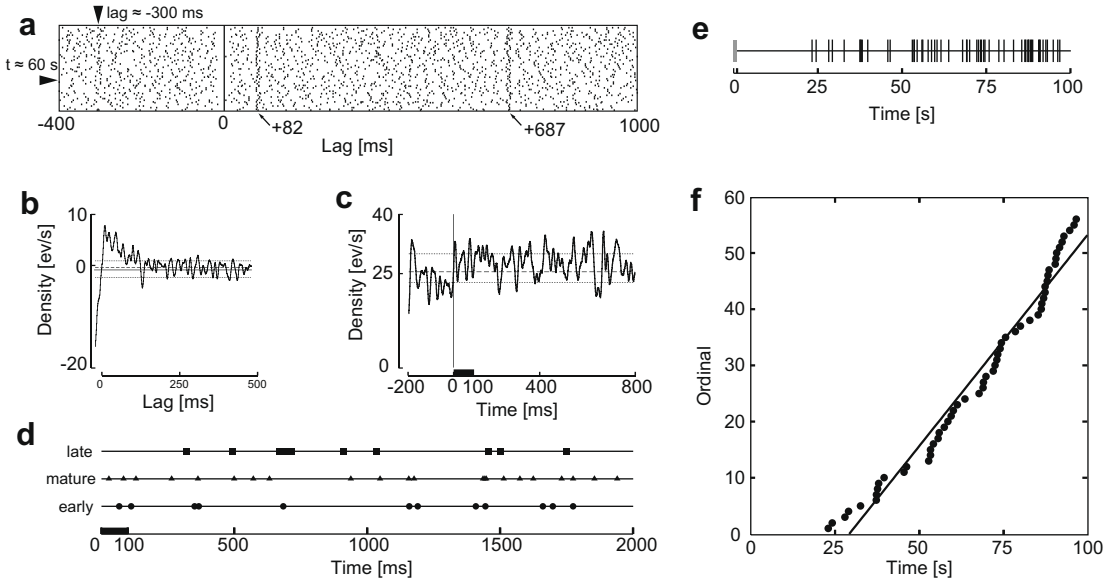

Fig. 9. Spatiotemporal firing pattern ⟨BDC, BDC, BDC; 82 ± 3.5, 687 ± 5.5⟩ that repeated 56 times in presence of apoptosis. Unit #BDC spontaneous mean firing rate: 23.3 spikes/s. Raster plot aligned on the pattern start (a), autocorrelogram (b), peri-event time histogram (c), peri-stimulus pattern plot (d), raster plot of pattern onset (e), and pattern occurrence regression plot (f). See Fig. 8 for more details of panels layout. Notice that at $t \approx 60,000$ ms the triplet tended to become a quadruplet with an additional event that appeared almost 300 ms before the current pattern onset.

It was an obvious observation that the introduction of apoptosis left less cells surviving at the arbitrary end of the simulation set at 100,000 time units. It was less obvious to observe that the average firing rate of the surviving cells was moderately increased (from 4.3 to 4.6 and 5.0 spikes/s with $T_{edp} = 700$ and $T_{edp} = 800$, respectively). These differences are probably due to the fact that the death of inhibitory cells due to apoptosis began about 70 time steps before the death of excitatory units. As a consequence, the excitatory/inhibitory (E/I) balance was modified such to leave a higher ratio of excitatory connections at the time STDP was enabled. Despite the overall decrease in number of excitatory connections the change of E/I balance is likely to be the cause of the increase in firing rate after apoptosis.

We recorded the spike trains of all excitatory units that were not directly receiving afferences from the external input and we searched for precise firing sequences that occurred beyond random expectation with the PGA algorithm (Tetko and Villa, 2001). The results show that after apoptosis the number of precise firing sequences was reduced but their structure and dynamics was modified.

Firstly, we observed more triplets than quadruplets after apoptosis. This is in agreement with most experimental results in this field (Abeles and Gerstein, 1988; Villa and Abeles, 1990; Abeles et al., 1993; Prut et al., 1998; Villa et al., 1999; Tetko and Villa, 2001; Ben-Shaul et al., 2004; Villa, 2005). The fact that more quadruplets than triplets were found in absence of apoptosis is prob-

ably due to the estimation procedure for pattern significance implemented by PGA. The procedure of PGA tended to underestimate triplets in order to emphasize the avoidance of detecting spurious precise firing sequences even if this would provoke the rejection of truly significant patterns. It is assumed that a significant pattern formed by four events (a quadruplet) should give birth to some significant triplets among its subpatterns. The rationale is that due to the "noisy" background activity embedded in the overall network activity there are less chances to detect a quadruplet than a triplet. In our simulations we are certainly far from implementing a background activity with natural characteristics and we do not have the "noise" introduced by the experimental spike sorting procedure.

Secondly, we observed a much higher number of repetitions of precise firing sequences after apoptosis (about 57 vs. 19, on average). This suggests that the firing patterns that emerge after apoptosis are likely to be more stable. This is a very important observation in view of attempting to raise an hypothesis of the functional outcome provoked by the death of exuberant cells and connections during neural development (Innocenti and Price, 2005). We assume that developmental and/or learning processes are likely to potentiate or weaken certain pathways through the network and let emerge cell assemblies characterized by precise firing sequences (Abeles, 1991). We suggested that the detection of such firing patterns could be associated with the emergence of functionally defined cell assemblies from the initially locally connected random network (Iglesias et al., 2005). The emerging connectivity within these cell assemblies would be the mean to preserve and process accurate temporal information within the network. The example reported in Fig. 9 suggests that the modifications in connectivity induced by cell death and synaptic pruning are part of a dynamical process that "builds up" as time runs and are therefore difficult to nail down.

There are evidence that feed-forward chains of neurons with diverging–converging connections may correspond to the topology of cell assemblies (Abeles et al., 2004) and we are investigating in this direction (Turova and Villa, 2007). However, there are also evidence suggesting that precise firing sequences might be controlled by attractors emerging out of the deterministic nonlinear dynamics of the network (Villa, 2000; Asai et al., 2006). The self-organization of spiking neurons into cell assemblies was reported in other studies of large simulated networks connected by STDP-driven projections (Izhikevich et al., 2004). These authors emphasized the emergence of spontaneously self-organized neuronal groups, even in absence of correlated input, associated with the spatiotemporal structure of firing patterns, if axonal conduction delays and STDP were included in the model. They suggest these self-organizing groups generate stereotypical patterns of activity with millisecond precision through a mechanism called "polychronization" (Izhikevich, 2006). In our view it is difficult to rule out one or another hypothesis at this stage. Further investigation is required in particular about the conditions necessary to support the emergence of a pattern of diverging–converging connections in the developing brain.

Our simulation results should be considered preliminary for many reasons. Among those we point out the fact we analyzed only a reduced number of simulation runs and we still need to investigate in depth the dynamics of the topological changes that occur in the developing network. There is an increasing interest in investigating the cortical circuits and their synaptic connectivity with a statistical approach related to graph theory (Chialvo, 2004; Sporns et al., 2004). Results obtained from layer 5 neurons in the visual cortex of developing rats indicate that many aspects of the connectivity patterns differ from random networks (Song et al., 2005). In particular, the distribution of synaptic connection strengths in those cortical circuits show an over-representation of strong synaptic connections correlated with the over-representation of some connectivity patterns. (Song et al., 2005) suggest that the local cortical network structure could be viewed as a skeleton of stronger connections in a sea of weaker ones.

In conclusion, we have presented new data to interpret the finding of precise firing sequences supported by a simulation framework of neural development. We have found evidence that apoptosis during early brain development is likely to play an essential role to let emerge cell assemblies that are more stable to sustain processing of temporal information. The framework that was presented here offers also the possibility to study the effect of genomic expressions patterns embedded in large spiking neural networks. This investigation will probably represent a complementary field of study to neural dynamics in an attempt to raise and test more refined hypotheses to understand information processing during neural development.

Acknowledgments

This work was partially funded by the European Community Future and Emerging Technologies Complex Systems program, Grant #034632 (PERPLEXUS), the European Community New and emering science and technology program, Grant #043309 (GABA) and the Swiss National Science Foundation SNF, Grant #PA002–115330/1.

References

Abeles, M., 1991. Corticonics: Neural Circuits of the Cerebral Cortex, first ed. Cambridge University Press.
Abeles, M., Gerstein, G.L., 1988. Detecting spatiotemporal firing patterns among simultaneously recorded single neurons. J. Neurophysiol. 60 (3), 910–924.
Abeles, M., Bergman, H., Margalit, E., Vaadia, E., 1993. Spatiotemporal firing patterns in the frontal cortex of behaving monkeys. J. Neurophysiol. 70, 1629–1638.
Abeles, M., Hayon, G., Lehmann, D., 2004. Modeling compositionality by dynamic binding of synfire chains. J. Computat. Neurosci. 17, 179–201.
Asai, Y., Yokoi, T., Villa, A.E.P., 2006. Detection of a dynamical system attractor from spike train analysis. Lect. Notes Comput. Sci. 4131, 623–631.
Bell, C.C., Han, V.Z., Sugawara, Y., Grant, K., 1997. Synaptic plasticity in a cerebellum-like structure depends on temporal order. Nature 387 (6630), 278–281.
Ben-Shaul, Y., Drori, R., Asher, I., Stark, E., Nadasdy, Z., Abeles, M., 2004. Neuronal activity in motor cortical areas reflect the sequential context of movement. J. Neurophysiol. 91, 1748–1762.
Bonfoco, E., Krainc, D., Ankarcrona, M., Nicotera, P., Lipton, S.A., 1995. Apoptosis and necrosis: two distinct events induced, respectively, by mild and intense insults with n-methyl-D-aspartate or nitric oxide/superoxide in cortical cell cultures. Proc. Natl. Acad. Sci. USA 92, 7162–7166.
Catalano, S.M., Shatz, C.J., 1998. Activity-dependent cortical target selection by thalamic axons. Science 281 (5376), 559–562.
Chechik, G., Meilijson, I., Ruppin, E., 1999. Neuronal regulation: a mechanism for synaptic pruning during brain maturation. Neural Computat. 11, 2061–2080.
Chen, B., Boukamel, K., Jao, J.P.Y., Roerig, B., 2005. Spatial distribution of inhibitory synaptic connections during development of ferret primary visual cortex. Exp. Brain Res. 160, 496–509.
Chialvo, D.R., 2004. Critical brain networks. Physica A 340, 756–765.
Choi, D.W., Koh, J.Y., Peters, S., 1988. Pharmacology of glutamate neurotoxicity in cortical cell culture: attenuation by nmda antagonists. J. Neurosci. 8, 185–196.
Conel, J.L., 1939–1963. The Post Natal Development of the Human Cerebral Cortex, vol. 6. Harvard University Press.
Cotman, C.W., Monaghan, D.T., 1988. Excitatory amino acid neurotransmission: nmda receptors and hebb-type synaptic plasticity. Annu. Rev. Neurosci 11, 61–80.
Draper, N.R., Smith, H., 1998. Applied Regression Analysis, third ed. Wiley, New York, NY.
Durbin, J., Watson, G.S., 1971. Testing for serial correlation in least squares regression. iii. Biometrika 58 (1), 1–19.
Egawa-Tsuzuki, T., Ohno, M., Tanaka, N., Takeuchi, Y., Uramoto, H., 2004. The pdgf b-chain is involved in the ontogenic susceptibility of the developing rat brain to nmda toxicity. Exp. Neurol. 186 (1), 89–98.
Elston, G.N., 2002. Cortical heterogeneity: implications for visual processing and polysensory integration. J. Neurocytol. 31, 317–335.
Eriksson, J., Torres, O., Mitchell, A., Tucker, G., Lindsay, K., Halliday, D., Rosenberg, J., Moreno, J.M., Villa, A.E.P., 2003. Spiking neural network for reconfigurable poetic tissue. Lect. Notes Comput. Sci. 2606, 165–173.

Figiel, I., Kaczmarek, L., 1997. Cellular and molecular correlates of glutamate-evoked neuronal programmed cell death in the in vitro cultures of rat hippocampal dentate gyrus. Neurochem. Int. 31, 229–240.
Fujita, I., 2002. The inferior temporal cortex: architecture, computation, and representation. J. Neurocytol. 31, 359–371.
Genoux, D., Montgomery, J.M., 2007. Glutamate receptor plasticity at excitatory synapses in the brain. Clin. Exp. Pharmacol. Physiol. 34 (10), 1058–1063.
Gerkin, R.C., Lau, P.M., Nauen, D.W., Wang, Y.T., Bi, G.Q., 2007. Modular competition driven by nmda receptor subtypes in spike-timing-dependent plasticity. J. Neurophysiol. 97, 2851–2862.
Guyonneau, R., Van Rullen, R., Thorpe, S.J., 2005. Neurons tune to the earliest spikes through stdp. Neural Computat. 17, 859–879.
Hanson, M.G., Landmesser, L.T., 2004. Normal patterns of spontaneous activity are required for correct motor axon guidance and the expression of specific guidance molecules. Neuron 43, 687–701.
Hill, S., Villa, A.E.P., 1997. Dynamic transitions in global network activity influenced by the balance of excitation and inhibition. Network: Computat. Neural Networks 8, 165–184.
Huttenlocher, P.R., 1979. Synaptic density in human frontal cortex – developmental changes and effects of aging. Brain Research 163 (2), 195–205.
Huttenlocher, P.R., Dabholkar, A.S., 1997. Regional differences in synaptogenesis in human cerebral cortex. J. Comp. Neurol. 387, 167–178.
Huttenlocher, P.R., de Courten, C., Garey, L.J., Van der Loos, H., 1982. Synaptogenesis in human visual cortex – evidence for synapse elimination during normal development. Neurosci. Lett. 33 (3), 247–252.
Iglesias, J., Villa, A.E.P., 2006. Neuronal cell death and synaptic pruning driven by spike-timing dependent plasticity. Lect. Notes Comput. Sci. 4131, 953–962.
Iglesias, J., Villa, A.E.P., 2007. Effect of stimulus-driven pruning on the detection of spatiotemporal patterns of activity in large neural networks. BioSystems 89, 287–293.
Iglesias, J., Eriksson, J., Grize, F., Tomassini, M., Villa, A.E.P., 2005. Dynamics of pruning in simulated large-scale spiking neural networks. BioSystems 79 (1), 11–20.
Iglesias, J., Eriksson, J., Pardo, B., Tomassini, M., Villa, A.E.P., 2005. Emergence of oriented cell assemblies associated with spike-timing-dependent plasticity. Lect. Notes Comput. Sci. 3696, 127–132.
Innocenti, G.M., 1995. Exuberant development of connections, and its possible permissive role in cortical evolution. Trends Neurosci. 18 (9), 397–402.
Innocenti, G.M., Price, D.J., 2005. Exuberance in the development of cortical networks. Nat. Rev. Neurosci. 6, 955–965.
Izhikevich, E.M., 2006. Polychronization: computation with spikes. Neural Computat. 18, 245–282.
Izhikevich, E.M., Gally, J.A., Edelman, G.M., 2004. Spike-timing dynamics of neuronal groups. Cereb. Cortex 14, 933–944.
Jiang, Q., Gu, Z., Zhang, G., Jing, G., 2000. N-methyl-D-aspartate receptor activation results in regulation of extracellular signal-regulated kinases by protein kinases and phosphatases in glutamate-induced apoptotic-like death. Brain Res. 887, 285–292.
Johnston, M.V., Trescher, W.H., Ishida, A., Nakajima, W., 2001. Neurobiology of hypoxic–ischemic injury in the developing brain. Pediatr. Res. 49, 735–741.
Karmarkar, U.R., Buonomano, D.V., 2002. A model of spike-timing dependent plasticity: one or two coincidence detectors? J. Neurophysiol. 88 (1), 507–513.
Kure, S., Tominaga, T., Yoshimoto, T., Tada, K., Narisawa, K., 1991. Glutamate triggers internucleosomal dna cleavage in neuronal cells. Biochem. Biophys. Res. Commun. 179, 39–45.
Levitt, P., 2003. Structural and functional maturation of the developing primate brain. J. Pediatr. 143, S35–S45.
Lopez-Bendito, G., Molnar, Z., 2003. Thalamocortical development: how are we going to get there? Nat. Rev. Neurosci. 4, 276–289.
Low, L.K., Cheng, H.J., 2006. Axon pruning: an essential step underlying the developmental plasticity of neuronal connections. Philos. Trans. Roy. Soc. 361 (1473), 1531–1544.
Luo, L., O'Leary, D.D., 2005. Axon retraction and degeneration in development and disease. Annu. Rev. Neurosci. 28, 127–156.
Mizuno, H., Hirano, T., Tagawa, Y., 2007. Evidence for activity-dependent cortical wiring: formation of interhemispheric connections in neonatal mouse visual cortex requires projection neuron activity. J. Neurosci. 27 (25), 6760–6770.
Montgomery, J.M., Madison, D.V., 2004. Discrete synaptic states define a major mechanism of synapse plasticity. Trends Neurosci. 27 (12), 744–750.
Oppenheim, R.W., 1981. Studies in developmental neurobiology: essays in honor of viktor hamburger. In: Cowan, W.M. (Ed.), The Neurotrophic Theory and Naturally Occurring Motoneuron Death. Oxford University Press, New York, NY.
Oppenheim, R.W., 1991. Cell death during development of the nervous system. Annu. Rev. Neurosci. 14, 453–501.
Press, W.H., Flannery, B.P., Teukolsky, S.A., Vetterling, W.T., 1992. Numerical Recipes in C: The Art of Scientific Computing, second ed. Cambridge University Press.
Prut, Y., Vaadia, E., Bergman, H., Slovin, H., Abeles, M., 1998. Spatiotemporal structure of cortical activity: properties and behavioral relevance. J. Neurophysiol. 79, 2857–2874.
Rakic, P., Bourgeois, J., Eckenhoff, M.F., Zecevic, N., Goldman-Rakic, P.S., 1986. Concurrent overproduction of synapses in diverse regions of the primate cerebral cortex. Science 232 (4747), 232–235.
Rakic, P., Bourgeois, J., Goldman-Rakic, P.S., 1994. Competitive interactions during neural and synaptic development. Prog. Brain Res. 102, 227–243.
Rice, D., Barone, S.J., 2000. Critical periods of vulnerability for the developing nervous system: evidence from humans and animal models. Environ. Health Persp. 108 (suppl. 3), 511–533.
Roberts, P.D., Bell, C.C., 2002. Spike timing dependent synaptic plasticity in biological systems. Biol. Cybern. 87, 392–403.
Sanchez, E., Perez-Uribe, A., Upegui, A., Thoma, Y., Moreno, J.M., Villa, A., Volken, H., Napieralski, A., Sassatelli, G., Lavarec, E., 2007. Perplexus: pervasive computing framework for modeling complex virtually-unbounded systems. In: AHS '07: Proceedings of the Second NASA/ESA Conference on Adaptive Hardware and Systems. IEEE Computer Society, Washington, DC, pp. 587–591.
Schelman, W.R., Andres, R.D., Sipe, K.J., Kang, E., Weyhenmeyer, J.A., 2004. Glutamate mediates cell death and increases the bax to bcl-2 ratio in a differentiated neuronal cell line. Mol. Brain Res. 128 (2), 160–169.
Shatz, C.J., 1990. Impulse activity and the patterning of connections during CNS development. Neuron 5 (6), 745–756.
Shmiel, T., Drori, R., Shmiel, O., Ben-Shaul, Y., 2006. Temporally precise cortical firing patterns are associated with distinct action segments. J. Neurophysiol. 96 (5), 2645–2652.
Song, S., Sjöström, P.J., Reigl, M., Nelson, S., Chklovskii, D.B., 2005. Highly nonrandom features of synaptic connectivity in local cortical circuits. Public Library Sci. Biol. 3 (3), 507–519.
Sporns, O., Chialvo, D.R., Kaiser, M., Hilgetag, C.C., 2004. Organization, development and function of complex brain networks. Trends Cogn. Sci. 8 (9), 418–425.
Tetko, I.V., Villa, A.E.P., 2001. A pattern grouping algorithm for analysis of spatiotemporal patterns in neuronal spike trains. 1. Detection of repeated patterns. J. Neurosci. Methods 105, 1–14.
Tetko, I.V., Villa, A.E.P., 2001. A pattern grouping algorithm for analysis of spatiotemporal patterns in neuronal spike trains. 2. Application to simultaneous single unit recordings. J. Neurosci. Methods 105, 15–24.
Turova, T.S., Villa, A.E.P., 2007. On a phase diagram for random neural networks with embedded spike timing dependent plasticity. BioSystems 89, 280–286.
Urakubo, H., Honda, M., Froemke, R.C., Kuroda, S., 2008. Requirement of an allosteric kinetics of nmda receptors for spike timing-dependent plasticity. J. Neurosci. 28, 3310–3323.
Villa, A.E.P., 2000. Time and the Brain. Harwood Academic. Volume 2.
Villa, A.E.P., 2005. Spatio-temporal patterns of spike occurrences in freely-moving rats associated to perception of human vowels. Auditory Cortex: Towards a Synthesis of Human and Animal Research. Lawrence Erlbaum Associates, New Jersey, pp. 241–254 (Chapter 17).
Villa, A.E.P., Abeles, M., 1990. Evidence for spatio-temporal firing patterns within the auditory thalamus of the cat. Brain Res. 509, 325–327.
Villa, A.E.P., Tetko, I., Hyland, B., Najem, A., 1999. Spatiotemporal activity patterns of rat cortical neurons predict responses in a conditioned task. Proc. Natl. Acad. Sci. USA 96, 1106–1111.
Yamamori, T., Rockland, K.S., 2006. Neocortical areas, layers, connections, and gene expression. Neurosci. Res. 55, 11–27.
Yuan, J., Lipinski, M., Degterev, A., 2003. Diversity in the mechanisms of neuronal cell death. Neuron 40, 401–413.
Zieminska, E., Stafiej, A., Lazarewicz, J.W., 2003. Role of group i metabotropic glutamate receptors and nmda receptors in homocysteine-evoked acute neurodegeneration of cultured cerebellar granule neurones. Neurochem. Int. 43, 481–492.